# *Aerogel-based solar thermal receivers*

# Aerogel-based solar thermal receivers

Kenneth McEnaney[a], Lee Weinstein[a], Daniel Kraemer[a], Hadi Ghasemi[b,*], Gang Chen[a,**]

[a] *Department of Mechanical Engineering, Massachusetts Institute of Technology, Cambridge, MA 02139, USA*
[b] *Department of Mechanical Engineering, University of Houston, Houston, TX 77204, USA*

**Abstract**

In any solar thermal application, such as solar space heating, solar hot water for domestic or industrial use, concentrating solar power, or solar air conditioning, a solar receiver converts incident sunlight into heat. In order to be efficient, the receiver must ideally absorb the entire solar spectrum while losing relatively little heat. Currently, state-of-the-art receivers utilize a vacuum gap above an absorbing surface to minimize the convection losses, and selective surfaces to reduce radiative losses. Here we investigate a receiver design that utilizes aerogels to suppress radiation losses, boosting the efficiency of solar thermal conversion. We predict that receivers using aerogels could be more efficient than vacuum-gap receivers over a wide range of operating temperatures and optical concentrations. Aerogel-based receivers also make possible new geometries that cannot be achieved with vacuum-gap receivers.

*Keywords:* solar receiver, solar thermal, aerogel

## 1. Introduction

Solar energy is abundant; the solar flux reaching the earth's surface is orders of magnitude larger than humankind's global power consumption[1]. Harvesting this energy requires enormous areal coverage, since the solar flux is very dilute.

*Corresponding author
**Principal corresponding author
*Email address:* gchen2@mit.edu (Gang Chen)

Photovoltaics harness this energy by converting sunlight directly into electricity. Many other processes rely on solar energy as a source of heat: the sun's energy can be used for space heating, heating hot water for domestic or industrial use[2], desalination[3], producing chemical fuels[4], heating a working fluid in a cycle to generate electricity[5], or driving other thermal energy conversion systems such as thermoelectric generators, thermionic generators, or thermophotovoltaics[6]. The sun's heat can even be used to drive air conditioning cycles[7]. In all of these processes, the solar radiation is absorbed as heat by a receiver, either in the form of an absorbing surface, a receiver cavity, or a volumetric absorber.

There has been extensive work developing receivers that strongly absorb sunlight without incurring large heat losses. One way is to introduce a solar optical concentrator in front of the receiver; the hot absorber surface can then be made smaller, which results in smaller heat losses to the environment. Common concentration schemes are linear Fresnel reflectors, which can concentrate the solar flux up to 40 times[8, 9]; linear parabolic troughs, which concentrate the solar flux by a factor of 30 to 60 onto a receiver tube[10]; heliostat fields, which can concentrate the solar flux by a factor of approximately 1,000 onto the receiver tower[11]; and parabolic dishes, which can concentrate the solar flux by a factor of approximately 10,000 onto the receiver at the dish's focus[12], or even higher if secondary optics are used[13].

There has also been extensive work on reducing losses from a receiver by modifying the receiver itself. Such methods include adding glass panes over the absorber surface to reduce convective losses[14]; placing the absorber in a vacuum enclosure to eliminate convective or conductive losses through the air[15]; and using an absorber with spectrally-selective properties to reduce the radiative losses in the infrared (IR) while still absorbing strongly over the solar spectrum[16, 17, 18]. Another method to reduce radiative losses is to introduce a radiation shield above the absorber[19]. Radiation shields are usually reflective metallic surfaces which reflect IR radiation back to the absorber. Radiation shields can also be designed to absorb the IR losses from the absorber and re-radiate at a lower temperature some of that heat back to the absorber. This

recycling of radiation reduces the overall rate of heat loss from the absorber. If a reflective or an absorbing radiation shield is placed in front of a solar absorber, the shield must also be transmissive to the solar spectrum such that the sunlight reaches the absorber. These selective transmitters can be as simple as a pane of glass[20], or complex such as a multilayer selective transmitter[21].

In some instances, more than one radiation shield has been used to reduce radiation losses. Each successive shield added reduces the overall heat loss. Taking this concept to the limit, one can imagine replacing many thin radiation shields with one continuous medium - a volumetric radiation shield. This volumetric radiation shield would need to be spectrally selective, allowing sunlight to pass while absorbing or reflecting IR radiation, and it would need to have low thermal conductivity such that the outer surface would be at a significantly lower temperature than the absorber.

We propose using aerogels as a volumetric radiation shield for a solar thermal receiver. Aerogels are low-density materials which can be transparent across the solar spectrum, opaque in the IR, and have a very low solid thermal conductivity[22]. By reducing heat losses while still having high solar transparency, aerogels allow a system to either operate at higher receiver efficiency, or allow the same receiver efficiency to be obtained at lower optical concentrations. They also are strong enough in compression such that they can be used in flat-panel architectures to support glass panes[23], which previously was not possible for vacuum-gap receivers. While modeling and experiments have been performed using aerogels as volumetric radiation shields for solar hot water systems[24, 25, 26], they have not been explored for higher-temperature systems. We will explore this regime in detail in this work.

Aerogels are low-density material foams most commonly produced through a sol-gel process[27]. Aerogels can be made from a variety of materials, such as silica[22], carbon[28], and various oxides[29]. The microscopic closed cellular structure of the aerogel prevents the gas currents responsible for macroscopic convection, and the low density means that there is very little material to pass heat via conduction. These properties make aerogels excellent insulators, al-

though at higher temperatures radiation within the aerogel can have a significant impact on the effective thermal conductivity. Aerogels can be naturally opaque or transparent to radiation. The properties of aerogels can be modified through seed inclusions such as oxide particles[30] or carbon-based flakes or rods[31]. They also are strongly dependent on the synthesis technique[32]. By choosing the right materials and process, aerogels can be achieved with desired performance characteristics for solar thermal receivers.

In this paper we model the performance of aerogel-based thermal receivers. First we provide an explanation of the concept, and a conceptual model with just the heat equation. Then we provide a detailed model for calculating performance using the coupled heat equation and equation of radiative transfer, similar to work in the literature on low-temperature systems[24]. Next, we provide an intermediate coupled model based on the Rosseland diffusion approximation[33]. Finally we compare the results of the models, and explore the potential for these receivers.

## 2. Concept

For any solar receiver, the receiver efficiency is defined as the fraction of the incident sunlight on the receiver, $Q_{s,rec}$, which is converted into heat and delivered to the thermal system below the absorber. Looking at the effective properties of the receiver as a whole, the efficiency can be expressed as:

$$\eta_{rec} = \frac{Q_h}{Q_{s,rec}} = \frac{Q_{abs} - Q_{loss}}{Q_{s,rec}} = \frac{Q_{abs} - Q_{loss}}{CQ_{sol}} \tag{1}$$

where $Q_h$ is the delivered heat, $Q_{abs}$ is the absorbed sunlight, and $Q_{loss}$ is the sum of all the thermal losses. In the denominator, the solar flux on the receiver is represented as the product of the standard solar flux (e.g. the AM1.5 Direct + Circumsolar value of 900 W/m$^2$), $Q_{sol}$, and an optical flux concentration ratio, $C$. The fraction of sunlight absorbed (and not reflected or scattered away) can be represented by an overall effective absorptance, $\alpha_{eff} = Q_{abs}/Q_{s,rec}$; then equation 1 can be rewritten as:

$$\eta_{rec} = \alpha_{eff} - \frac{Q_{loss}}{CQ_{sol}} \tag{2}$$

High solar absorption, small thermal losses, and high optical concentration all contribute to a high receiver efficiency.

Figure 1 is a schematic of our proposed aerogel-based receiver. Unconcentrated or concentrated light is incident on the receiver. Some of the sunlight is lost due to reflections at the interfaces and within the aerogel. Most of the radiation emitted by the absorber is absorbed by the aerogel and re-emitted back to the absorber, thus reducing the radiation loss from the absorber. The parasitic conduction loss through the aerogel is very small due to the low solid thermal conductivity of the aerogel. The heat loss is conducted through the glass and lost to the environment via radiation and convection.

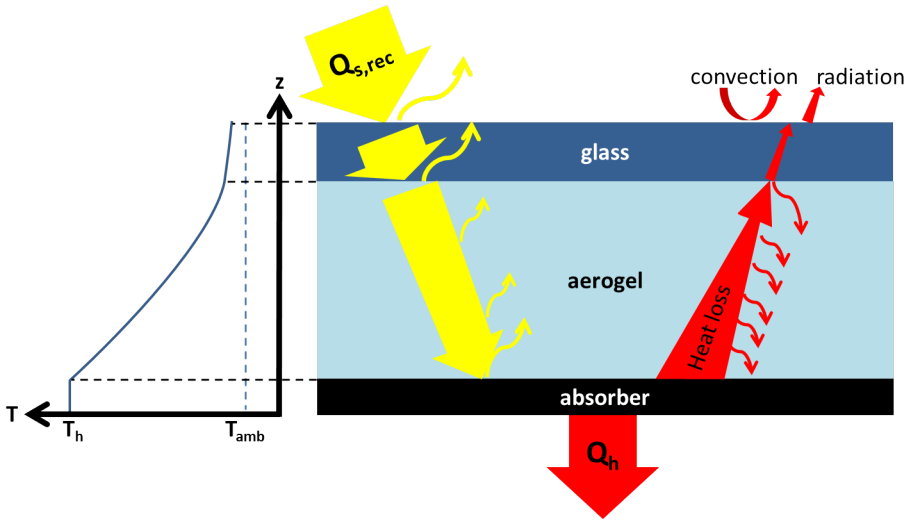


Figure 1: Schematic of an aerogel-based receiver. There are some reflections at the interfaces and within the aerogel that diminish the amount of sunlight reaching the absorber. The aerogel acts as a volumetric radiation shield: much of the radiation from the absorber is absorbed by the aerogel and reemitted back to the absorber. Some heat loss reaches the glass, where it is conducted to the top surface and lost to the environment via convection and radiation.

## 3. Conceptual Model

In the ideal case, the volumetric radiation shield is good enough to suppress all radiation from the absorber; the only heat loss from the absorber is via conduction through the aerogel. The amount of sunlight that is transmitted through the aerogel is a decaying exponential function of the aerogel thickness. With these two basic concepts we can calculate the receiver efficiency:

$$\eta_{rec} = \frac{Q_{s,rec}\tau_g e^{-\alpha_a L_a}\alpha_{abs} - k_a \frac{T_h - T_{g,i}}{L_a}}{Q_{s,rec}} \tag{3}$$

where $\tau_g$ is the transmittance of the glass, $\alpha_a$ is the effective absorptance of the aerogel, $L_a$ is the thickness of the aerogel, $\alpha_{abs}$ is the absorptance of the absorber, and $k_a$ is the solid thermal conductivity of the aerogel. The temperature of the inner surface of the glass, $T_{g,i}$, can be solved by balancing the heat flux through the glass with the convective and radiative losses to the environment:

$$k_g \frac{T_{g,i} - T_{g,o}}{L_g} = h\left(T_{g,o} - T_{amb}\right) + \sigma_{sb}\epsilon_g\left(T_{g,o}^4 - T_{amb}^4\right) \tag{4}$$

where $k_g$ is the thermal conductivity of the glass, $T_{g,o}$ is the temperature of the outer surface of the glass, $L_g$ is the thickness of the glass, $h$ is the convective heat transfer coefficient, $T_{amb}$ is the ambient temperature, $\sigma_{sb}$ is the Stefan-Boltzmann constant, and $\epsilon_g$ is the IR emittance of the glass. As we can see from equation 3, as the aerogel thickness is decreased, the amount of sunlight absorbed by the receiver increases, but the thermal losses through the aerogel increase. This simple analysis suggests there is an optimal aerogel thickness to maximize receiver efficiency, which balances the aerogel transmittance with the thermal conduction losses through the aerogel.

In the preceding ideal model, all radiation from the absorber was suppressed. However, this is not realistic; all wavelengths of radiation will penetrate the aerogel to some depth. To properly solve the heat transfer within the aerogel-based receiver we must use a more detailed model based on the equation of radiative transfer. This detailed model is presented in the following section.

## 4. Detailed Model

To more accurately capture the radiation effects within the aerogel, the equation of radiative transfer is solved. The equation of radiative transfer states that the radiative intensity in a specific direction inside a medium is decreased due to absorption and out-scattering, and increased due to thermal emission and in-scattering from all other angles[33]:

$$\cos\theta \frac{\mathrm{d}I_{\Omega'}}{\mathrm{d}z} = -\left(\kappa + s\right) I_{\Omega'} + \kappa I_b + \frac{s}{4\pi} \int_{4\pi} \Phi_{\Omega\to\Omega'} I_\Omega \,\mathrm{d}\Omega \tag{5}$$

where $I_{\Omega'}$ is the intensity in a given direction, $\theta$ is the polar direction away from $z$, $\kappa$ is the absorption coefficient, $s$ is the scattering coefficient, $I_b$ is the blackbody intensity at a position $z$, and $\Phi_{\Omega\to\Omega'}$ is the phase function from angle $\Omega$ into $\Omega'$. We assume aerogels scatter isotropically, meaning the phase function is 1[34, 35, 36, 37]. The properties of aerogels are strongly wavelength-dependent (Fig. 2), so the equation of radiative transfer should be solved for each wavelength of light. To make the problem computationally tractable, we divide the radiation spectrum into N bands, and assume that across each band the absorption and scattering coefficients are constant. For our calculations, we divided the spectrum into 11 bands. For a given band $i$ between wavelengths $\lambda_i$ and $\lambda_{i+1}$ the blackbody intensity must be weighted by the fraction of the blackbody spectrum in that band:

$$\cos\theta \frac{\mathrm{d}I_{i,\Omega'}}{\mathrm{d}z} = -\left(\kappa_i + s_i\right) I_{i,\Omega'} + \kappa_i I_{bi} + \frac{s_i}{4\pi} \int_{4\pi} I_{i,\Omega} \,\mathrm{d}\Omega \tag{6}$$

where

$$I_{b,i} = n^2 \sigma_{sb} T_z^4 \frac{15}{\pi^4} \int_{C_2/n\lambda_2 T_z}^{C_2/n\lambda_1 T_z} \frac{\xi^3}{e^\xi - 1} \,\mathrm{d}\xi \tag{7}$$

The constant $C_2 = 0.014388$ m K. For each band, the heat flux in the $z$-direction is:

$$q_{z,i} = \int_{4\pi} I_{i,\Omega} \cos\theta \, \mathrm{d}\Omega \tag{8}$$

The radiative heat flux must be solved in conjunction with the solid conduction in the aerogel. The gradient of the summed radiative heat fluxes is inserted as a source term in the heat equation:

$$0 = k_a \frac{\mathrm{d}^2 T}{\mathrm{d}z^2} + \frac{\mathrm{d}}{\mathrm{d}z} \sum_{i=1}^{N} q_{z,i} \tag{9}$$

At the absorber ($z = 0$) boundary, the temperature is fixed at the absorber temperature $T = T_h$; the radiation propagating in the positive z-direction ($I^+_{\Omega,i}$) is the sum of the radiation emitted from the absorber, and a reflected fraction of the radiation incident on the absorber:

$$I^+_{\Omega,i}(z = 0) = \epsilon_{abs,i} I_{b,i}(T_h) + (1 - \epsilon_{abs,i}) I^-_{\Omega,i}(z = 0) \tag{10}$$

where $\epsilon_{abs,i}$ is the average emittance of the absorber surface over the band $i$, and $I^-_{\Omega,i}$ is the radiation traveling in the opposite direction of $I^+_{\Omega,i}$. The glass is also treated with the equation of radiative transfer. The radiation in the aerogel just inside the interface with the glass ($z = L_a^-$) traveling away from the interface is the sum of radiation from the aerogel reflected off the interface and radiation within the glass transmitted through the interface:

$$I^-_{\Omega,i}(z = L_a^-) = R_{12,\Omega,i} I^+_{\Omega,i}(z = L_a^-) + T_{12,\Omega,i} I^-_{\Omega',i}(z = L_a^+) \tag{11}$$

where $R_{12,\Omega,i}$ and $T_{12,\Omega,i}$ are the reflectance and transmittance coefficients for the glass and aerogel interface at a given angle and band. These coefficients are calculated with the Fresnel equations for complex media[38]. The angle of travel within the aerogel, $\Omega$, is related to the angle of travel within the glass, $\Omega'$, with Snell's Law. The same procedure is used to calculate the radiation at the interface between the glass and the air:

$$I^{-}_{\Omega',i}(z=(L_a{+}L_g)^{-}) = R_{23,\Omega',i} I^{+}_{\Omega',i}(z=(L_a{+}L_g)^{-}){+}T_{23,\Omega,i}\left(I_{b,i}(T_{amb}) + I_{sol,\Omega,i}\right) \tag{12}$$

The solar intensity is assumed to be uniform within a half-angle of 2.9° and has the AM1.5 Direct + Circumsolar spectral intensity[39]. These equations are solved iteratively, until the temperature profiles and heat fluxes within the aerogels converge.

Silica aerogels, like typical glass, show strong absorption beyond 2.5 $\mu$m[40]. This is ideal as an insulator, since large IR absorption results in less heat transfer through the aerogel. The IR absorptance of silica aerogels is purely a function of the optical thickness of the aerogel, which is the product of the thickness of the material and its density, so absorptance results for a given density can be linearly scaled to find the properties at a different density. Figure 2 shows the measured extinction (absorption plus scattering) of various silica aerogels, normalized by their densities [32, 41, 42, 43, 40].

Unlike fully dense silica, silica aerogels scatter in the visible wavelengths. This scattering has been shown to be nearly isotropic[35, 36] and inversely proportional to the fourth power of the wavelength[34], characteristic of Rayleigh scattering of small particles or voids. This trend is illustrated in Figure 2. It has been shown that for a given density, the pore structure of the aerogel and hence its scattering is a strong function of the manufacturing process[32, 44]. Shown in Figure 2 is the bulk extinction of three aerogels produced with different processes but all having nearly the same density (80 kg/m$^3$)[32].

For these calculations, we assume that the aerogel extinction at wavelengths shorter than 1 $\mu$m is entirely due to scattering, and the extinction at wavelengths longer than 1 $\mu$m is entirely due to absorption. For the bands longer than 2 $\mu$m, the wavelength-dependent properties (from [41]) are averaged with equal weighting. For the bands shorter than 2 $\mu$m where the solar spectrum dominates the radiative transfer, the wavelength-dependent properties (from [32], pH=13) are averaged using the solar spectrum as the weighting.

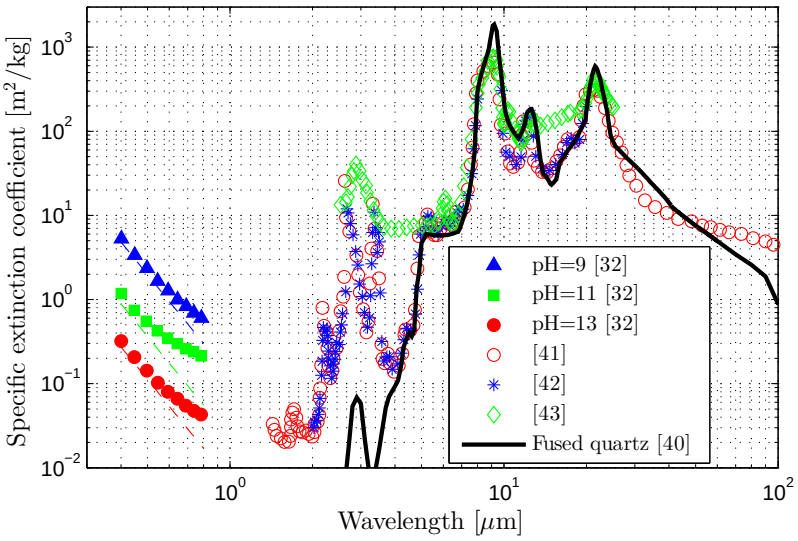


Figure 2: Measured specific extinction coefficient of silica aerogels. Solid black line shows the specific absorption coefficient of fused quartz[40]. Filled markers show scattering measurements of three silica aerogel samples with density 80 kg/m$^3$; the accompanying dashed lines show the bulk scattering coefficient (after the surface scattering has been subtracted)[32]. Markers without lines show measured specific absorption coefficients of silica aerogels[41, 42, 43]. The authors of [43] posit that the large absorption they measure in the 4 $\mu$m to 5 $\mu$m range is due to their samples containing water.

The real part of the index of refraction of aerogels is assumed to be independent of wavelength, and is obtained with the formula $n = 1 + (2.1 \times 10^{-4})\rho$ from literature[45], where the density is measured in kg/m$^3$. The imaginary part of the index of refraction is extracted from the absorption data[46]. The wavelength-dependent index of refraction of glass (fused quartz) is from literature[40]. The band averages for the glass were computed with the same weighting method as described for the aerogels.

## 5. Diffusion Model

In some situations, the heat transfer within the aerogel can be calculated with a more simple model based on the Rosseland diffusion approximation. In this model, the heat transfer in the aerogel layer is assumed to be one-dimensional and the temperature distribution in this layer is calculated by using the Rosseland diffusion approximation of radiative heat transfer. For a control volume in this layer, the heat equation is expressed as:

$$\rho c \frac{\partial T}{\partial t} = \frac{\partial q_{cond}}{\partial z} + \frac{\partial q_{rad}}{\partial z} \tag{13}$$

where $\rho$ denotes the density of the aerogel, $c$ the specific heat capacity of the aerogel, $T$ the local temperature inside the aerogel, $t$ the time, $q_{cond}$ the conductive heat flux density per unit area, $z$ the vertical coordinate and $q_{rad}$ the radiative heat flux per unit area. Based on the Rosseland approximation $q_{rad}$ can be expressed as

$$q_{rad} = -\left(\frac{16n^2\sigma_{sb}}{3\left(\alpha_a(T) + s\right)}T^3\right)\frac{\partial T}{\partial z} \tag{14}$$

where $n$ denotes the refractive index, $\alpha_a(T)$ the effective temperature-dependent absorption coefficient of the aerogel and $s$ the scattering coefficient of the aerogel. The general solution for the non-linear heat equation in the glass and aerogel layers is written as

$$z = \frac{1}{C_1}\int g(T)dT + C_3 \tag{15}$$

where

$$g(T) = \left( k_a + \frac{A}{\alpha_a(T) + s} T^3 \right) \tag{16}$$

with

$$A = \frac{16 n^2 \sigma_{sb}}{3} \tag{17}$$

and $C_1$ and $C_3$ are constants. Note that $g(T)$ and $A$ are different for the aerogel and glass layers.

For given thermal and optical properties of the aerogel layer and glass, $g(T)$, one can pose the boundary conditions to determine the temperature field in each layer. The transmission in the aerogel layer, as discussed, is expressed as a decaying exponential function. The boundary conditions are same as above (the fixed absorber temperature, the equality of conductive and radiative flux at the glass-aerogel interface, and the convective and radiation flux condition at the glass-air interface). The solution of the heat equation is applied to both the aerogel layer and the glass slab simultaneously to determine the temperature at the aerogel-glass interface, and the glass-air interface. The heat flux to the ambient from the cold side of the receiver and the receiver efficiency are calculated as defined in equation 1 but considering transmission losses in both the glass and aerogel layers.

## 6. Results

The three described models were used to calculate the maximum solar receiver efficiency and corresponding optimum aerogel thickness over a wide range of concentrations at two different operational temperatures: 100 °C, which is representative of domestic hot water systems, and 400 °C, which is a common operational temperature for solar thermal plants[47]. In addition to the aerogel and glass properties shown in figure 2, we use a glass thickness of 2 mm and thermal conductivity of 1 W/m/K; an ambient temperature of 25 °C; a convective heat transfer coefficient of 10 W/m$^2$/K; and an aerogel solid thermal

conductivity of 0.005 W/m/K. The thickness of the aerogel layer was limited to 50 mm for computational purposes; it was also deemed a reasonable upper bound for a practical manufacturing limit. The properties in figure 2 give the glass an effective solar transmittance of 93.1%.

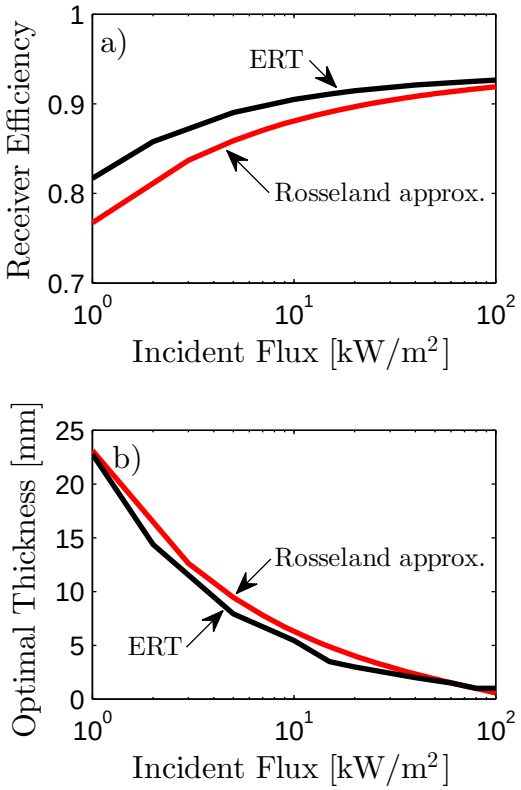


Figure 3: Performance of an aerogel-based receiver with an absorber temperature of 100 °C. a) Efficiency and b) optimal aerogel thickness, as calculated by the two different models. At this absorber temperature, the models agree reasonably well.

Figures 3 and 4 show the receiver efficiency as a function of concentration for two different absorber surface temperatures: 100 °C and 400 °C. The general trend is that the models are closest in agreement when the predicted optical thickness of the aerogel is small. This is not surprising: the main difference between the models is the treatment of the aerogel and glass, so if there is little

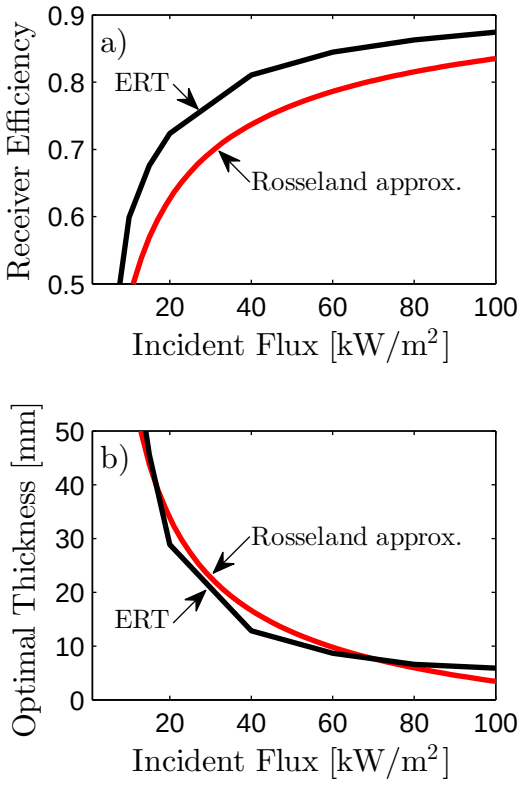


Figure 4: Performance of an aerogel-based receiver with an absorber temperature of 400 °C. a) Efficiency and b) optimal aerogel thickness, as calculated by the two different models. At this absorber temperature, the Rosseland approximation underestimates the efficiency.

aerogel then there should be little difference in the models' predictions.

In order to understand how the aerogel-based receiver performs compared to other receiver types, we calculate with the ERT model the receiver efficiency for three different receiver scenarios: 1) a blackbody absorber surface below a glass pane, with a vacuum gap between (denoted "bb/vacuum"); 2) a blackbody absorber surface below a glass pane, with aerogel between (denoted "bb/aerogel"; and 3) a wavelength-selective absorber surface below a glass pane, with a vacuum gap between (denoted "ss/vacuum"). The wavelength-dependent emittance of the selective surface is assumed to be a step function, with an emittance of 0.95 at wavelengths shorter 2 $\mu$m, and 0.05 at wavelengths longer than 2 $\mu$m. The receiver calculation results are shown in Figures 5 and 6.

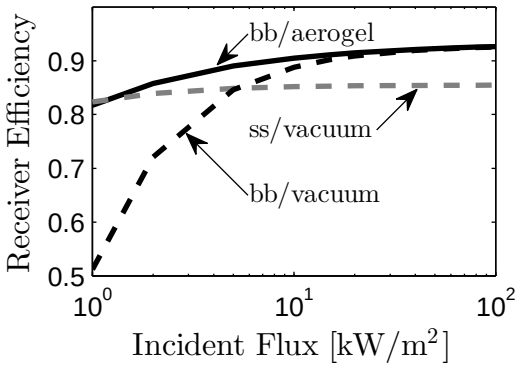


Figure 5: Efficiency of three different receivers with an absorber temperature of 100 °C: blackbody surface under an aerogel; blackbody surface under a vacuum; and a selective surface ($\epsilon$=0.95 for $\lambda < 2\,\mu$m; $\epsilon = 0.05$ for $\lambda > 2\,\mu$m) under a vacuum. The blackbody and aerogel receiver is the highest-performing.

We can see that for the 100 °C receiver, at high concentration aerogels make very little difference, and blackbody absorbers are the most efficient. Due to the low temperature and high optical concentration, the receiver efficiency is mainly determined by the solar absorption. Thus, aerogels and selective surfaces are not helpful because they increase solar reflection. At lower incident fluxes, aerogel-and-blackbody absorbers give the highest receiver efficiency because thermal

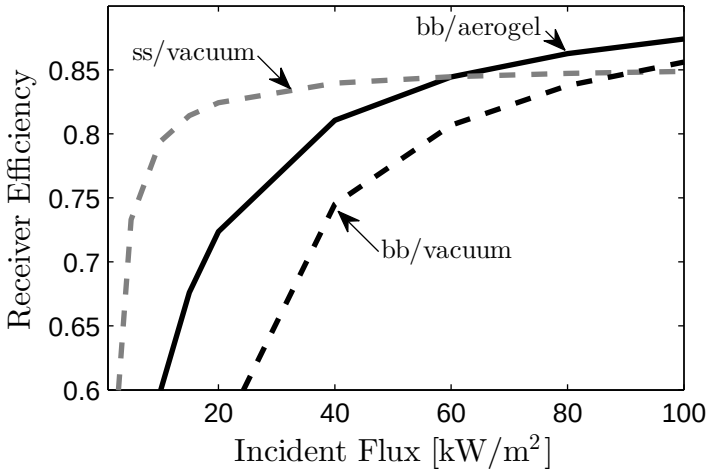


Figure 6: Efficiency of three different receivers with an absorber temperature of 400 °C: blackbody surface under an aerogel; blackbody surface under a vacuum; and a selective surface ($\epsilon$=0.95 for $\lambda < 2\,\mu$m; $\epsilon = 0.05$ for $\lambda > 2\,\mu$m) under a vacuum. The selective surface under vacuum is the highest-performing at moderate concentrations; at concentrations 60X or greater, the receiver comprising a blackbody and aerogel outperforms the other receivers.

losses determine the device performance, although there is not much difference compared to a selective surface under vacuum.

At an operating temperature of 400 °C, thermal losses become even more significant. Thus at low concentrations the selective surfaces outperform any blackbody receiver. The aerogel-and-blackbody receiver performs well at higher concentrations because the absorption is most important in this regime. In addition, at these high temperatures the stability of materials is critical, and stable, inexpensive black paints may be more reliable than multilayer selective surfaces.

A final note on these results is that we did not include the performance of a system comprising both a selective surface and an aerogel; this is because such a system is rarely optimal. The selective surface naturally loses little heat via radiation, so adding an aerogel only makes a small incremental reduction in the loss. With the accompanying drop in solar transmission, the net effect is a decrease in system performance compared to a selective surface and vacuum system. The only instance where a selective surface and aerogel system outperforms the other options is for high-temperature, non-concentrating applications, but in such an application all the systems described in this paper would have efficiencies less than 50%, so we consider them all to be unpractical.

## 7. Conclusion

Our models predict that for low- to mid-temperature applications at incident fluxes less than 100 suns, receivers comprising blackbody absorbers and aerogels are at least as efficient as current state-of-the-art selective surface evacuated receivers. These aerogel-based receivers could supplant traditional evacuated tube receivers, such as those used for high-efficiency domestic hot water and solar thermal troughs; reliability and cost will be the deciding factors. Because they do not need to be evacuated, aerogel-based receivers could bring the high efficiency normally associated with evacuated tube receivers to additional form-factor receivers such as flat panels.

## 8. Acknowledgments

K.M. and L.W. were supported by the ARPA-E FOCUS program (DE-AR0000471); D.K. was supported by the Department of Energy's SunShot program (DE-EE0005806). H.G. thanks the Natural Sciences and Engineering Research Council of Canada (NSERC) for their support.

## References

[1] N. S. Lewis, Toward cost-effective solar energy use, Science 315 (5813) (2007) 798–801. doi:10.1126/science.1137014.

[2] Renewables 2014 global status report, Tech. rep., Renewable Energy Policy Network for the 21st Century (2014).

[3] J. H. Lienhard, M. A. Antar, A. Bilton, J. Blanco, G. Zaragoza, Solar desalination, in: Annual Review of Heat Transfer, Begell House, 2012, pp. 277–347.

[4] A. Steinfeld, Thermochemical production of syngas using concentrated solar energy, in: Annual Review of Heat Transfer, Begell House, 2012, pp. 255–275.

[5] M. T. Dunham, B. D. Iverson, High-efficiency thermodynamic power cycles for concentrated solar power systems, Renewable and Sustainable Energy Reviews 30 (2014) 758–770. doi:10.1016/j.rser.2013.11.010.

[6] K. McEnaney, D. Kraemer, G. Chen, Direct heat-to-electricity conversion of solar energy, in: Annual Review of Heat Transfer, Begell House, 2012, pp. 179–230.

[7] C. A. Balaras, G. Grossman, H.-M. Henning, C. A. Infante Ferreira, E. Podesser, L. Wang, E. Wiemken, Solar air conditioning in Europe — an overview, Renewable and Sustainable Energy Reviews 11 (2) (2007) 299–314. doi:10.1016/j.rser.2005.02.003.

[8] S. A. Kalogirou, Solar thermal collectors and applications, Progress in Energy and Combustion Science 30 (3) (2004) 231 – 295. doi:10.1016/j.pecs.2004.02.001.

[9] G. Zhu, T. Wendelin, M. J. Wagner, C. Kutscher, History, current state, and future of linear fresnel concentrating solar collectors, Solar Energy 103 (2014) 639 – 652. doi:10.1016/j.solener.2013.05.021.

[10] Solar trough systems, Tech. rep., National Renewable Energy Laboratory (1998).

[11] A. Kribus, P. Doron, R. Rubin, J. Karni, A multistage solar receiver: The route to high temperature, Solar Energy 67 (1999) 3–11. doi:10.1016/S0038-092X(00)00056-6.

[12] T. Mancini, P. Heller, B. Butler, B. Osborn, W. Schiel, V. Goldberg, R. Buck, R. Diver, C. Andraka, J. Moreno, Dish-stirling systems: An overview of development and status, Journal of Solar Energy Engineering 125 (2003) 135–151. doi:10.1115/1.1562634.

[13] A. Lewandowski, C. Bingham, J. O'Gallagher, R. Winston, D. Sagie, Performance characterization of the SERI high-flux solar furnace, Solar Energy Materials 24 (14) (1991) 550–563. doi:10.1016/0165-1633(91)90090-8.

[14] K. G. T. Hollands, J. L. Wright, C. G. Granqvist, Glazings and coatings, in: J. Gordon (Ed.), Solar Energy - The State of the Art, 1st Edition, James and James Ltd, London, 2001, Ch. 2, pp. 29–108.

[15] M. Roesle, V. Coskun, A. Steinfeld, Numerical analysis of heat loss from a parabolic trough absorber tube with active vacuum system, Journal of Solar Energy Engineering 133 (2011) 031015. doi:10.1115/1.4004276.

[16] H. Tabor, Selective radiation. I: wavelength discrimination, Bulletin of the Research Council of Israel 5A (2) (1956) 119–128.

[17] F. Cao, K. McEnaney, G. Chen, Z. Ren, A review of cermet-based spectrally selective solar absorbers, Energy and Environmental Science 7 (2014) 1615–1627. doi:10.1039/C3EE43825B.

[18] P. Bermel, J. Lee, J. D. Joannopoulos, I. Celanovic, M. Soljačić, Selective solar absorbers, in: Annual Review of Heat Transfer, Begell House, 2012, pp. 231–254.

[19] L. Weinstein, D. Kraemer, K. McEnaney, G. Chen, Optical cavity for improved performance of solar receivers in solar-thermal systems, Solar Energy 108 (2014) 69–79. doi:10.1016/j.solener.2014.06.023.

[20] M. Telkes, Solar thermoelectric generators, Journal of Applied Physics 25 (6) (1954) 765–777. doi:10.1063/1.1721728.

[21] C. M. Lampert, Coatings for enhanced photothermal energy collection II. non-selective and energy control films, Solar Energy Materials 2 (1979) 1–17. doi:10.1016/0165-1633(79)90026-1.

[22] J. Fricke, T. Tillotson, Aerogels: production, characterization, and applications, Thin Solid Films 297 (1-2) (1997) 212–223. doi:10.1016/S0040-6090(96)09441-2.

[23] K. I. Jensen, J. M. Schultz, F. H. Kristiansen, Development of windows based on highly insulating aerogel glazings, Journal of Non-Crystalline Solids 350 (2004) 351–357. doi:10.1016/j.jnoncrysol.2004.06.047.

[24] A. Nordgaard, W. A. Beckman, Modelling of flat-plate collectors based on monolithic silica aerogel, Solar Energy 49 (5) (1992) 387–402. doi:10.1016/0038-092X(92)90111-M.

[25] S. Svendsen, Solar collector with monolithic silica aerogel, Journal of Non-Crystalline Solids 145 (1992) 240–243. doi:10.1016/S0022-3093(05)80464-8.

[26] K. Duer, S. Svendsen, Monolithic silica aerogel in superinsulating glazings, Solar Energy 63 (4) (1998) 259–267. doi:10.1016/S0038-092X(98)00063-2.

[27] S. S. Kistler, Coherent expanded aerogels and jellies, Nature 127 (1931) 741. doi:10.1038/127741a0.

[28] R. W. Pekala, Organic aerogels from the polycondensation of resorcinol with formaldehyde, Journal of Materials Science 24 (1989) 3221–3227. doi:10.1007/BF01139044.

[29] N. Hüsing, U. Schubert, Aerogels — airy materials: Chemistry, structure, and properties, Angewandte Chemie International Edition 37 (1-2) (1998) 22–45. doi:10.1002/(SICI)1521-3773(19980202)37:1/2<22::AID-ANIE22>3.0.CO;2-I.

[30] J. Wang, J. Kuhn, X. Lu, Monolithic silica aerogel insulation doped with $TiO_2$ powder and ceramic fibers, Journal of Non-Crystalline Solids 186 (1995) 296–300. doi:10.1016/0022-3093(95)00068-2.

[31] J. Fricke, X. Lu, P. Wang, D. Büttner, U. Heinemann, Optimization of monolithic silica aerogel insulants, International Journal of Heat and Mass Transfer 35 (9) (1992) 2305–2309. doi:10.1016/0017-9310(92)90073-2.

[32] A. Beck, G. Popp, A. Emmerling, J. Fricke, Preparation and characterization of $SiO_2$ two-step aerogels, Journal of Sol-Gel Science and Technology 2 (1994) 917–920. doi:10.1007/BF00486376.

[33] M. Modest, Radiative Heat Transfer, 2nd Edition, Academic Press, Boston, 2003.

[34] A. Emmerling, R. Petricevic, A. Beck, P. Wang, H. Scheller, J. Fricke, Relationship between optical transparency and nanostructural features of silica aerogels, Journal of Non-Crystalline Solids 185 (3) (1995) 240–248. doi:10.1016/0022-3093(95)00021-6.

[35] A. Beck, R. Caps, J. Fricke, Scattering of visible light from silica aerogels, Journal of Physics D: Applied Physics 22 (1989) 730–734. doi:10.1088/0022-3727/22/6/002.

[36] K. Kamiuto, S. Saitoh, Y. Tokita, Scattering phase function of a silica aerogel at 450 nm wavelength, Journal of Quantitative Spectroscopy and Radiative Transfer 50 (3) (1993) 293–299. doi:10.1016/0022-4073(93)90079-W.

[37] R. Stangl, M.-A. Einarsrud, W. Platzer, V. Wittwer, Optical characterization of silica xerogel with spectral and angle-dependent resolution, Solar Energy Materials and Solar Cells 54 (1-4) (1998) 181–188. doi:10.1016/S0927-0248(98)00069-5.

[38] G. Chen, Nanoscale Energy Transfer and Conversion, Oxford University Press, USA, 2005.

[39] Reference solar spectral irradiances: Direct normal and hemispherical on 37° tilted surface, Tech. Rep. ASTM Standard G 173-03, ASTM International (2008).

[40] R. Kitamura, L. Pilon, M. Jonasz, Optical constants of silica glass from extreme ultraviolet to far infrared at near room temperature, Applied Optics 46 (33) (2007) 8118–8133. doi:10.1364/AO.46.008118.

[41] U. Heinemann, R. Caps, J. Fricke, Radiation-conduction interaction: an investigation on silica aerogels, International Journal of Heat and Mass Transfer 39 (10) (1996) 2115–2130. doi:10.1016/0017-9310(95)00313-4.

[42] M. Reim, G. Reichenauer, W. Körner, J. Manara, M. Arduini-Schuster, S. Korder, A. Beck, J. Fricke, Silica-aerogel granulate — structural, optical and thermal properties, Journal of Non-Crystalline Solids 350 (2004) 358–363. doi:10.1016/j.jnoncrysol.2004.06.048.

[43] G. Wei, Y. Liu, X. Zhang, X. Du, Radiative heat transfer study on silica aerogel and its composite insulation materials, Journal of Non-Crystalline Solids 362 (2013) 231–236. doi:10.1016/j.jnoncrysol.2012.11.041.

[44] W. Cao, A. J. Hunt, Improving the visible transparency of silica aerogels, Journal of Non-Crystalline Solids 176 (1) (1994) 18–25. doi:10.1016/0022-3093(94)90206-2.

[45] S. Henning, L. Svensson, Production of silica aerogel, Physica Scripta 23 (1981) 697–702. doi:10.1088/0031-8949/23/4B/018.

[46] R. Siegel, J. Howell, Thermal Radiation Heat Transfer, 4th Edition, Taylor & Francis, New York, 2002.

[47] D. Kearney, U. Herrmann, P. Nava, B. Kelly, R. Mahoney, J. Pacheco, R. Cable, N. Potrovitza, D. Blake, H. Price, Assessment of a molten salt heat transfer fluid in a parabolic trough solar field, Journal of Solar Energy Engineering 125 (2) (2003) 170. doi:10.1115/1.1565087.